https://doi.org/10.5194/egusphere-2025-2305
Preprint. Discussion started: 28 May 2025

Global modeling of brown carbon: impact of temperature- and humidity-dependent bleaching

Xinchun Xie[1,2,3], Yuzhong Zhang[2,3*], Ruosi Liang[1,2,3], Xuan Wang[4]

[1] College of Environmental and Resource Sciences, Zhejiang University, Hangzhou, Zhejiang 310058, China

[2] Key Laboratory of Coastal Environment and Resources of Zhejiang Province, School of Engineering, Westlake University, Hangzhou, Zhejiang 310030, China

[3] Institute of Advanced Technology, Westlake Institute for Advanced Study, Hangzhou, Zhejiang 310024, China

[4] School of Energy and Environment, City University of Hong Kong, Kowloon Tong 999077 Hong Kong SAR, China;

Correspondence to: Yuzhong Zhang (zhangyuzhong@westlake.edu.cn)

https://doi.org/10.5194/egusphere-2025-2305
Preprint. Discussion started: 28 May 2025

Abstract: Brown carbon (BrC), a light-absorbing component of organic aerosols, undergoes bleaching in the atmosphere, a process where its light-absorption capacity diminishes over time. A recent study suggests that the lifetime of fresh BrC against bleaching (τ_{BrC}) is influenced by ambient temperature and relative humidity. In this study, we incorporate the improved τ_{BrC} parameterization into the atmospheric chemical transport model (GEOS-Chem) to assess its impact on atmospheric chemistry and radiative effects. Our results show that τ_{BrC} varies strongly with altitude, ranging from 1–10 hours in the planetary boundary layer (PBL) to over 100 hours in the upper troposphere, where bleaching becomes negligible. Dry regions (e.g., Northern Africa, South Asia) exhibit longer surface τ_{BrC}, while humid regions (e.g., tropics) show shorter τ_{BrC}. The updated τ_{BrC} parameterization triples global fresh BrC burdens compared to the baseline parameterization with uniform τ_{BrC}, increasing its effective lifetime from 0.45 to 1.45 days and amplifying its direct radiative effect (DRE) by 48% (from +0.059 to +0.088 W m^{-2}). Lofted wildfire emissions experience prolonged τ_{BrC} due to reduced bleaching in the free troposphere, underscoring the importance of fire injection height. Additionally, BrC absorption suppresses photochemical activity, reducing JNO_2 by up to 7.4%, surface ozone by 0–2.5% and tropospheric OH by 0–6.9%. These effects intensify during major wildfire events, such as Siberian fires in 2019 that caused JNO_2 and ozone to drop by 36.3% and 17.5%, respectively, highlighting BrC's role in perturbing atmospheric oxidation capacity.

Keywords: Brown carbon, bleaching lifetime, biomass burning, direct radiative effect, atmospheric chemistry

https://doi.org/10.5194/egusphere-2025-2305
Preprint. Discussion started: 28 May 2025

1. Introduction

Brown carbon (BrC), a highly complex and dynamic mixture of organic aerosols (Lin et al., 2017), is notable for its ability to absorb sunlight in the ultraviolet (UV) and visible wavelengths, contributing to the warming of the atmosphere (Washenfelder et al., 2015; Andreae and Gelencsér, 2006; Laskin et al., 2015). Previous studies indicate that BrC accounts for 7–19% of total aerosol light absorption (Feng et al., 2013), with its influence reaching up to 40–50% at 300–400 nm wavelengths (Lack and Langridge, 2013). The atmospheric radiative forcing due to BrC can be as much as 40% of that caused by black carbon (BC) (Srinivas et al., 2016), and approximately 24% in the troposphere (Zhang et al., 2017).

Biomass burning emissions are the primary source of global BrC (Andreae and Merlet, 2001; Andreae and Gelencsér, 2006), contributing ~60% of BrC warming effect (Yue et al., 2022), followed by contributions from residential wood combustion and agricultural burning (Saleh et al., 2014). Frequent and intensive wildfire events, driven by climate change, land-use practices, and natural variability (Fu et al., 2013; Jolly et al., 2015), have raised the concerns of positive feedback through wildfires (Zheng B et al., 2023 ; Cunningham et al., 2024). Large-scale fires emit substantial amounts of aerosols, adversely affecting global climate, human health and the economy, reversing the downward trend in global $PM_{2.5}$ levels (Li et al., 2023; Burke et al., 2023), and significantly impacting the Earth's radiation balance (Huang et al., 2023).

Only a few current global climate and aerosol radiative forcing models account for the light absorption of organic carbon (OC) in the near-UV to visible range, most models still treat BC as the only significant light-absorbing aerosol (Kelesidis et al., 2022). Studies have shown that the direct forcing effect (DRE) from BrC around +0.1 W m^{-2}, corresponding to about 25% of the BC (0.39 W m^{-2}) (Zhang et al., 2020). Collow et al. (2024) first introduced BrC as an independent aerosol component in the GOCART-2G model, using an e-folding time of 1 day, and found that including BrC significantly

https://doi.org/10.5194/egusphere-2025-2305
Preprint. Discussion started: 28 May 2025

improved simulated absorption in the ultraviolet band. What more, Feng et al. (2013) demonstrated that the radiative effect of organic aerosols in certain regions of the tropopause could shift from cooling (–0.08 W m^{-2}) to warming (+0.025 W m^{-2}) when BrC is included in radiative simulations, a result consistent with Delessio et al. (2024), who reported a BrC DRE of 0.04 W m^{-2} in the GISS ModelE. Srinivas et al. (2016) found that BrC accounts for 40% of the atmospheric radiative forcing caused by BC, and Chung et al. (2012) estimated that 20% of the solar radiation absorption by carbonaceous aerosols at 550 nm originates from BrC. When BrC bleaching is considered, the reported global DRE values are reduced to 0.06 W m^{-2} (Brown et al., 2018) and 0.029 W m^{-2} (Drugé et al., 2022). This warming effect of carbonaceous aerosols in the tropopause is especially evident in regions with significant biomass burning.

BrC primarily absorbs light in the near UV-visible spectrum, reducing sunlight availability for photolysis reactions. This absorption alters the local photochemical environment, reducing the photolysis of nitrogen dioxide (NO_2) to nitric oxide (NO) - a crucial step in ozone formation, leading to lower ozone levels in regions with high BrC concentrations. Other free radicals (e.g., OH and HO2) are similarly affected (Wu et al., 2019). OH radicals, which are key atmospheric oxidants, are primarily generated through the reaction between $O(^1D)$ (produced by UV-induced ozone decomposition) and water molecules. Studies have shown that BrC emissions from biomass burning can reduce OH concentrations by 5–30% in affected areas (Hammer et al., 2016). While the effects of BrC on atmospheric oxidation are currently underexplored (Selimovic et al., 2020), further investigation is essential to understand its climate implications.

Atmospheric BrC evolve through photochemical aging, where exposure to sunlight and atmospheric oxidants modifies its chemical structure and optical properties. Over short timescales, BrC can darken near its source, while bleaching and oxidative whitening occur over longer timescales (e.g., a day or more after emission). The bleaching time

https://doi.org/10.5194/egusphere-2025-2305
Preprint. Discussion started: 28 May 2025

(referred to as lifetime in this study) of BrC is a critical factor that influences its climatic impact, but it remains challenging to quantify accurately. Accurately parameterizing the lifetime of BrC in climate models is essential for predicting its distribution, concentration, and radiative effects. Most studies simplify BrC's lifetime to either exclude bleaching or assume a constant value of about one day (Feng et al., 2013; Jo et al., 2016; Wang et al., 2018). However, wildfire-driven convective vertical transport can extend BrC's lifetime, as particle viscosity affects its atmospheric persistence (Schnitzler et al., 2022; Xu et al., 2024). The lifetime in the upper troposphere is significantly longer than one day, and there are also differences in different dimensional bands (Schnitzler et al., 2022). Neglecting these variations leads to inaccurate estimates of BrC's effects in models.

In this study, we update the bleaching lifetime parameterization of BrC in the model and examine the impacts of this update on the radiative effects of wildfire-derived BrC. Unlike BC, whose climate impacts are relatively well understood, BrC's atmospheric warming effect remains highly variable and poorly represented in climate models. Given the expected increase in wildfire activity globally, quantifying BrC's radiative impacts is becoming increasingly critical. This study investigates the influence of wildfire emissions on the distribution and optical properties of atmospheric BrC, integrates updates to BrC's bleaching lifetime, accounts for wildfire emission heights, and explores the extensive effects of BrC on regional and global chemical processes as well as its climate impact.

2. Method

2.1 GEOS-Chem simulation

The global simulations utilize version 12-8 of GEOS-Chem with a horizontal resolution of 4 ° × 5 ° and 47 vertical levels, which is driven by meteorology fields from the Modern Era Retrospective-analysis for Research and Applications, version 2 (MERRA-2) (Gelaro et al., 2017) (https://gmao.gsfc.nasa.gov/reanalysis/MERRA-2/, Last access: 20 February, 2024).

https://doi.org/10.5194/egusphere-2025-2305
Preprint. Discussion started: 28 May 2025

The Rapid Radiative Transfer Model for Global Circulation Models (RRTMG) is a widely used radiative transfer model in climate and atmospheric research. It calculates both longwave and shortwave radiative fluxes and heating rates in the atmosphere, which are essential for understanding climate dynamics. RRTMG is invoked every three hours to compute instantaneous atmospheric radiative fluxes at 30 wavelengths within the spectrum from 0.23 to 56 μm with clear sky(Heald et al., 2014). By coupling RRTMG with GEOS-Chem, the direct radiative forcing (DRF) can be calculated to study the climatic effects of BrC.

The global anthropogenic emission inventory uses EDGARv43 (Crippa et al., 2018). Canada is replaced by APEI (Canada, 2016), the USA is replaced by NEI (2014), Asia is replaced by MIX (Li et al., 2017), and regional Africa is replaced by DICE_Africa (Marais and Wiedinmyer, 2016). The biofuel emissions are from Bond et al. (2007) emission inventory. Daily resolved biomass burning emissions of BC and POA are from the Global Fire Emissions Database with small fires (GFED4s) (Giglio et al., 2013; Van Der Werf et al., 2017; Randerson et al., 2017). The BC/OC in GFED4s is 0.11.

In the model, all fire emissions are set by default within the planetary boundary layer (PBL), and we have added an additional setting in this experiment, which is to assume that 65% of fire emissions are within the boundary layer. These two experimental settings are coincident with the BrC lifetime settings. After all, the total OC emissions were 42.74 Tg, and BC emissions were 8.24 T in 2019. The total BrC emissions were 27.46 Tg, of which biomass burning emission was 21.17 Tg.

In this model, POA is derived from simulated primary OC by applying an OA/OC mass ratio of 2.1(Wang et al., 2018). SOA is modeled using the simple scheme based on established methods(Kim et al., 2015; Pye et al., 2010). For primary emissions, the model specifies that 80% of BC, 50% of anthropogenic OC, and 50% of biomass

https://doi.org/10.5194/egusphere-2025-2305
Preprint. Discussion started: 28 May 2025

burning OC are initially hydrophobic. These hydrophobic aerosols convert to hydrophilic forms, which are subject to wet removal, with an e-folding time of 1.2 days(Park, 2003). All SOA aerosols are considered as hydrophilic. The formation of sulfate-nitrate-ammonium aerosols is detailed in previous studies(Shah et al., 2020; Shao et al., 2019), and their thermodynamic equilibrium is computed using the ISORROPIA II (Fountoukis and Nenes, 2007). Dust aerosols and sea salt aerosols are simulated according to Duncan Fairlie et al. (2007) and Jaeglé et al. (2011). In this study, the BC and OA are treated as externally mixed as described in Wang et al. (2014), the absorption enhancement for fossil BC is 1.1, and 1.5 for biofuel and biomass burning BC.

2.2 Brown carbon simulation

The BrC optical properties are implemented following Wang et al. (2018). All organic aerosols freshly emitted from biomass and biofuel burning are treated as BrC. Our approach is functionally equivalent to simulating an external mixture of purely scattering organic aerosols and absorptive organic aerosols, provided that the mass absorption efficiency (MAE) of BrC is defined as the average of the MAE of organic aerosols and absorptive organic aerosols weighted by their mass fractions. Although there is some observational evidence, mainly in China, that primary organic aerosols from fossil fuel combustion are light absorbing (Yan et al., 2017; Chen et al., 2020), their contribution is relatively small on the global scale and we assume that fossil fuel POA is non-absorbing.

The MAE at different wavelengths is computed based on the Mie theory, as a function of aerosol size, aerosol density, and the refractive index. The size of OA is assumed to follow a log-normal distribution, with a geometric median diameter of 180 nm and a standard deviation of 1.6 (Wang et al., 2018). The density of OA is set at 1.3 g cm^{-3}. The real part of the refractive index is 1.5, while the imaginary part and its wavelength dependence are parameterized based on the mass emission ratios of BC/OA [50]. The BC/OA ratios are specified as 0.05 for biomass burning and 0.12 for biofuel,

https://doi.org/10.5194/egusphere-2025-2305
Preprint. Discussion started: 28 May 2025

representing average global burning conditions (Wang et al., 2018). The Mie calculations based on these parameters yield an MAE of 1.3 m^2 g^{-1} for biomass burning aerosols and 1.2 m^2 g^{-1} for biofuel aerosols at the 365 nm wavelength, with corresponding absorption Ångström exponents (AAE) of 3.1 and 2.6 between 300 and 600 nm.

To account for the reduction in absorption due to photo-bleaching, we assume that the absorption of chemically aged BrC is 1/4 of that of freshly emitted BrC, resulting in an MAE of 0.37 m^2 g^{-1} for bleached biomass burning aerosols and 0.30 m^2 g^{-1} for biofuel burning aerosols at 365 nm.

Wang et al. (2018) specified the rate of BrC chemical aging to be $\frac{[OH]}{5\times10^5}$ d^{-1} where [OH] is the OH concentration in molec·cm^{-3}. This yields roughly a chemical lifetime of about one day against photo-bleaching, generally consistent with field observations in the lower troposphere (Wang et al., 2018; Forrister et al., 2015). A recent study by Schnitzler et al. (2022) found in laboratory experiments that the chemical lifetime of BrC increases substantially with enhanced particle viscosity when temperature and RH get lower. In this study, we implement the parameterization of BrC chemical lifetime (τ_{BrC}, in s) developed by Schnitzler et al. (2022), which depends on ambient temperature (T) and relative humidity (RH) following Eq. (1):

$$\tau_{BrC} = A\,[D_0(T)\left(\frac{\eta_0(T)}{\eta_{\mathrm{BrC}}(T,RH)}\right)^{\xi}]^{-\frac{1}{2}} \quad (1)$$

D_0 is the diffusion rate of ozone in pure water, calculated with the Stokes-Einstein equation as a function of T. η_0 is the viscosity of pure water as a function of T, and η_{BrC} is the viscosity of aqueous BrC aerosols, parameterized as a function of T and RH based on the experimental measurements (Schnitzler et al., 2022). A and ξ are treated as constants where A=0.125 m $s^{-1/2}$ and ξ =0.684. The chemical lifetime of BrC is calculated and updated online in the GEOS-Chem simulation driven by T and RH data from MERRA-2.

https://doi.org/10.5194/egusphere-2025-2305
Preprint. Discussion started: 28 May 2025

2.3 Observational data

We use observations from aircraft campaigns (ATom mission, Figure S1) and a ground-based remote sensing network (AERONET) to evaluate our simulations of BrC. The Atmospheric Tomography Mission (ATom) is a NASA-led aircraft campaign aimed at measuring and understanding the global distribution of greenhouse gases and reactive gases and aerosols (Thompson et al., 2022). The ATom flights, conducted between 2016 and 2018, sampled extensive latitudinal and longitudinal ranges, from the Arctic to the Antarctic and over both the Pacific and Atlantic Oceans (Prather et al., 2017). During the ATom -2, ATom -3, and ATom -4, BrC was sampled at altitudes ranging from 0.2 to 12 km aboard the NASA DC-8 aircraft, alongside a comprehensive suite of gases and aerosols. Water-soluble BrC (WS BrC) in aerosols was measured with three systems: a spray chamber (MC) coupled to a liquid waveguide capillary cell (LWCC), and a particle-into-liquid sampler (NOAA PILS-LWCC) coupled to an LWCC (Washenfelder et al., 2015). The MC-LWCC system collects aerosols through a spray chamber, trapping the particles in water, which are then analyzed using an LWCC and a spectrometer. The PILS-LWCC system collects aerosols into a liquid stream for similar analysis. The detection limits at 365 nm were 1.53 Mm^{-1} (MC), 0.89 Mm^{-1} (CSU), and 0.03 Mm^{-1} (NOAA), respectively. A factor of 2 is used to convert the light absorption of BrC in solution to the light absorption of atmospheric particles (Liu et al., 2013; Zhang et al., 2017). In this study, we evaluate our simulations against the measurements taken during ATom -4, which occurred from April 24 to May 21, 2018 (https://espoarchive.nasa.gov/archive/browse/atom/id14/DC8, Last access: 25 October, 2024). Samples were collected every 5 minutes at altitudes below 3 km and every 15 minutes at higher altitudes, yielding a total of 1,074 samples. The flight path in ATom-4 is shown in Figure S1.

The AERONET (AErosol RObotic NETwork) program is a federation of ground-based remote sensing aerosol networks established by NASA and LOA-PHOTONS (CNRS) (Holben et al., 2006). The program provides a long-term, continuous and readily accessible public domain database of aerosol optical, microphysical and radiative

https://doi.org/10.5194/egusphere-2025-2305
Preprint. Discussion started: 28 May 2025

properties. AERONET's aerosol optical depth (AOD) observations are derived from direct solar radiation in multiple wavelength bands, mainly ranging from 340 nm to 1640 nm, while other aerosol properties (including single scattering albedo SSA and absorbing aerosol optical depth AAOD) are derived from diffuse sky radiation at four wavelengths: 440, 675, 870 and 1020 nm (Dubovik and King, 2000). This study extracted AOD and AAOD at 440 nm from AERONET data in 2019 to compare with the model simulation results. We use high-quality Level 2.0 AOD data (uncertainty of 0.01 in the visible range and 0.02 in the ultraviolet range (Giles et al., 2019) and quality-controlled Level 1.5 almucantar inversion AAOD data.

2.4 Simulation experiments

We perform a series of global 4°×5° GEOS-Chem simulations for 2019 to examine the impact of environmental-condition-dependent BrC chemical lifetime (τ_{BrC}) on the abundance and distribution of BrC globally. To test the impact of vertical partitioning of fire emissions and its interactions with τ_{BrC} parameterizations, we perform GEOS-Chem simulations that assign 100% (0%) and 65% (35%) of wildfire emissions in the boundary layer (free troposphere). In addition to 2019, but we also run the April and May 2018 simulation to evaluate against the ATom -4 observations. In addition, we use the GFED5 beta version to test biomass emission sensitivity.

Table 1. descriptions of model sensitivity experiments.

Experiments	Lifetime	Emission inventory	Fire emissions fraction under PBL
Base	original τ_BrC	GFED4s	100%
BaFt	original τ_BrC	GFED4s	65%
Upd	Updated τ_BrC	GFED4s	100%
UpdFt	Updated τ_BrC	GFED4s	65%
UpdGF5	Updated τ_BrC	GFED5	100%

3. Results and Discussion

3.1 Chemical lifetime of BrC against bleaching

Figure 1 shows the spatial distribution of τ_{BrC} as parameterized based on Schnitzler et

https://doi.org/10.5194/egusphere-2025-2305
Preprint. Discussion started: 28 May 2025

al (Schnitzler et al., 2022). In the planetary boundary layer (< 1.5 km), τ_{BrC} is roughly 1 – 10 hours, indicating that BrC's light-absorbing capacity rapidly degrades on the timescale of a day, generally consistent with ground or lower troposphere observations (Laskin et al., 2015; Forrister et al., 2015). τ_{BrC} increases dramatically with altitude, driven primarily by decreased temperature. τ_{BrC} reaches $10^{2.5}$ hours ≈ 2 weeks in the mid-troposphere at ~ 4 km, comparable to the lifetime of aerosols against wet and dry deposition. At higher altitude, τ_{BrC} further increases by several orders of magnitude, rendering photo-bleaching effectively negligible in the upper troposphere, which is supported by a few analyses of high-altitude measurements (Liu et al., 2014; Zhang et al., 2017).

In addition to vertical variations, τ_{BrC} also varies considerably across different regions of the globe (Figure S2a). The horizontal variations at the same altitude appear to be controlled mainly by relative humidity (Figure S2). At the surface and the lower troposphere, τ_{BrC} tends to be several days longer in dry regions such as Northern Africa, Middle Asia, Western U.S., Northern Australia, Southern Africa, and Southern America. In the free troposphere, τ_{BrC} is shorter in the Inter-Tropical Convergence Zone because of the higher humidity due to convective updrafts.

In contrast, the [OH] dependent parameterization of τ_{BrC} implemented in Wang et al. (Wang et al., 2018) exhibits much smaller spatial variations, predicting τ_{BrC} to be on the order of a day throughout the troposphere. The [OH] dependent parameterization was constructed based on very few field studies, mostly in lower troposphere conditions (Forrister et al., 2015). The two parameterizations predict similar τ_{BrC} in the planetary boundary layer but differ greatly in the middle and upper troposphere. These differences would have important implications for the global distribution and the radiative impact of primary organic aerosols from biomass and biofuel burning.

https://doi.org/10.5194/egusphere-2025-2305
Preprint. Discussion started: 28 May 2025

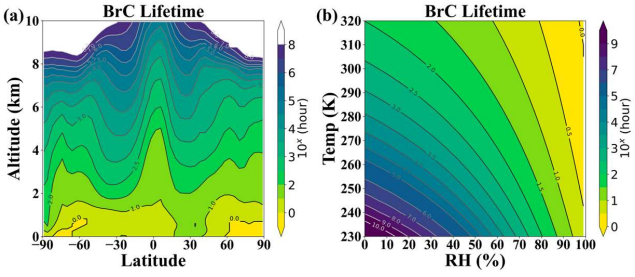

Figure 1. The lifetime of BrC as a function of altitude and latitude(a) and as a function of Temperature and relative humidity(b).

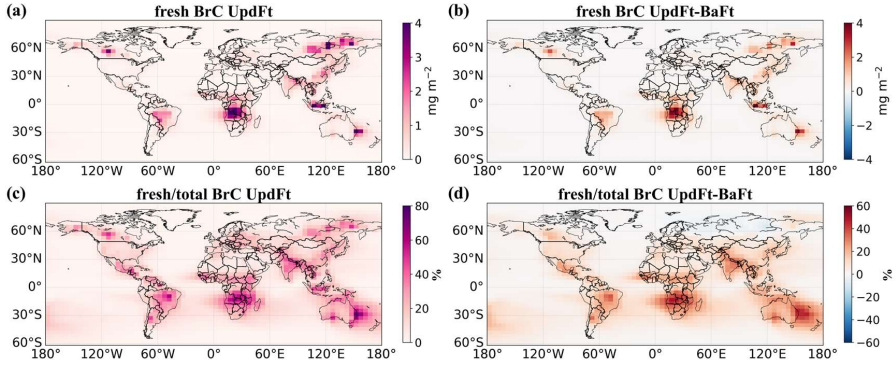

Figure 2. (a) Global distribution of fresh BrC column density with updated τ_BrC, (b) Difference of fresh BrC column density between updated τ_BrC and original τ_BrC, (c) fresh to total BrC column density distribution with updated τ_BrC, (d) Difference of fresh to total BrC column density distribution with updated τ_BrC and original τ_BrC at surface.

https://doi.org/10.5194/egusphere-2025-2305
Preprint. Discussion started: 28 May 2025

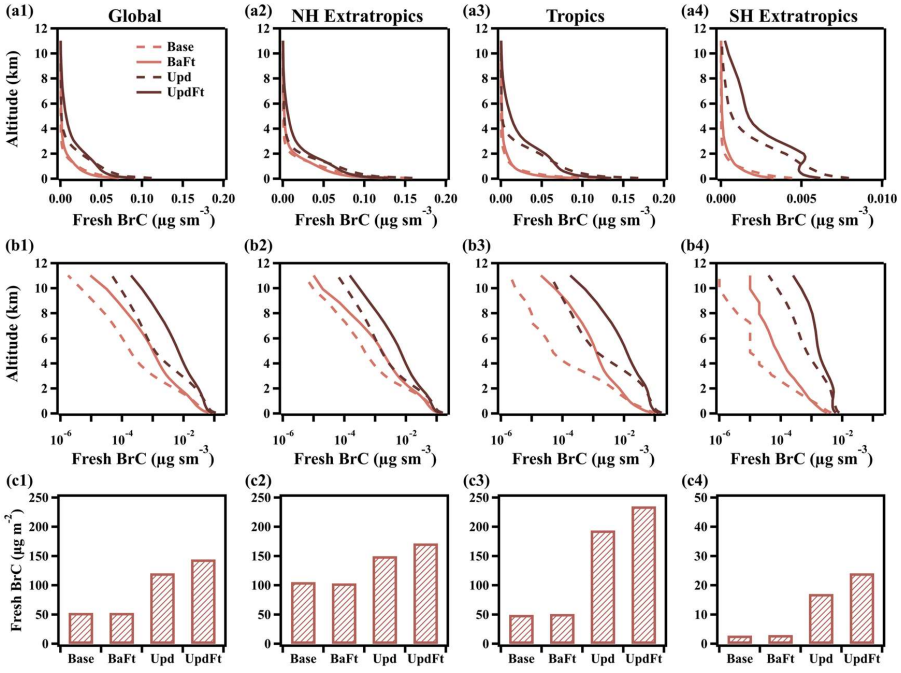

Figure 3. Vertical profiles and column densities of fresh BrC concentrations in the Northern Hemisphere Extratropics, Tropics, and Southern Hemisphere Extratropics simulated by the GEOS-Chem model.

3.2 Global distribution of fresh BrC

Figure 2a shows the global distribution of fresh BrC column density in 2019, which reveals elevated concentrations in regions characterized by substantial biomass burning and biofuel emissions (Figure S3). These hotspots include tropical Africa (biomass), tropical South America (biomass), East Siberia (biomass), South Asia (biofuel), and East China (biofuel). Compared to the baseline simulation, the updated simulation with temperature- and RH-dependent τ_{BrC} yields higher fresh BrC concentrations across most regions. The largest increase is observed in southern Africa, which is due to long τ_{BrC} near the surface (Figure 1) resulting from the region's strong biomass burning emissions (Figure S3) and dry environmental conditions (Figure S2). Conversely, despite intensive wildfire emissions in East Siberia, the updated simulation shows

https://doi.org/10.5194/egusphere-2025-2305
Preprint. Discussion started: 28 May 2025

minimal differences in fresh BrC concentrations because of comparable τ_{BrC} values between the two parameterizations (Figure S2a).

Figure 3 compares the vertical profiles and average column densities of fresh BrC concentrations across simulations. The updated simulation (UpdFt), with revised τ_{BrC} and fire injection parameterizations, yields the highest fresh BrC concentrations, with average column densities of 235 μg m^{-2} in the tropics, 172 μg m^{-2} in the Northern Extratropics, and 24 μg m^{-2} in the Southern Extratropics. These values represent factors of 4.7, 1.6, 8.6 increases, respectively, compared to the baseline simulation. Globally, the updated simulation (UpdFt) produces an average column density of 144 μg m^{-2}, three times that of the baseline simulation (53 μg m^{-2}). Given the global average emission fluxes of BrC, this result translates to an effective τ_{BrC} of 1.45 days in the UpdFt simulation, as compared to 0.45 days in the baseline simulation.

Vertical profiles of fresh BrC demonstrate significant differences between the UpdFt and baseline simulations. The absolute differences are particularly large in the lower troposphere of the tropics, reaching up to 0.05 μg m^{-3}, while relative differences are most pronounced in the upper troposphere, exceeding a factor of 10 despite lower absolute concentrations. Meanwhile, the τ_{BrC} parameterization will not change the total BrC concentrations (fresh + bleached BrC) (Figure S4(a)), as the abundance of total BrC is controlled by the rate of wet and dry deposition.

The influence of τ_{BrC} parameterization on fresh BrC concentrations is modulated by fire emission injection height. Direct injection of emissions into the free troposphere results in slower BrC bleaching and higher concentrations at elevated altitudes. Simulations incorporating 35% of fire emissions injected into the free troposphere (Thapa et al., 2022) show 30-50% greater fresh BrC burdens compared to those with emissions confined to the surface layer (Figure 3), underscoring the interactions between τ_{BrC} and fire injection mechanisms.

https://doi.org/10.5194/egusphere-2025-2305
Preprint. Discussion started: 28 May 2025

Figure S4(b) shows the vertical distribution of the ratio between the absorption coefficient of BrC (BrC-Abs_{440}) and BC (BC-Abs_{440}) at 440 nm. It can be observed that the absorption coefficient of fresh BrC increases by approximately a factor of 4.3. Moreover, the absorption of BrC becomes stronger with increasing altitude, highlighting the significant role of BrC light absorption in the upper atmosphere (Zhang et al., 2017).

3.3 Evaluation against observations

We compare our simulations with the aircraft campaign ATom-4 which measured the global distribution of BrC over remote oceans (Figure S1) (Zeng et al., 2020). The baseline simulation severely underestimates BrC absorption at 365 nm (Abs_{365}) (Figure 4a). The updated simulation with longer τ_{BrC} increases fresh BrC concentrations and hence their Abs_{365} by about an order of magnitude, bringing the simulation results closer to but still lower than the observations (Figure 4a). Meanwhile, the model generally captures observed levels of OA and CO during ATom-4, but with an underestimation of OA in the upper troposphere and an overestimation of CO in the lower troposphere (Figure 4).

We also compare our simulations to ground-based AERONET observations, which measures AOD and AAOD at 440 nm across global continents (Figure 5). The model well reproduces both the magnitude and the distribution of observed AOD, with R= 0.80 and mean bias = 0.02. Meanwhile, the model underestimates high AAOD observed in regions with strong influence of biomass burning, such as Africa, South America, and Siberia. It well captures high AAOD observed in southern and eastern Asia, where the absorption is mainly due to BC from anthropogenic sources. Overall, the baseline simulation achieves a R of 0.69 and a mean bias of -0.0085 against AERONET AAOD observations (Figure 6). The updated τ_{BrC} parameterization does not notably improve this comparison (Figure 6). It is important to note that only level 2 AAOD data from

https://doi.org/10.5194/egusphere-2025-2305
Preprint. Discussion started: 28 May 2025

AERONET are used in this study. Due to the absence of AAOD retrievals under low-AOD conditions (AOD < 0.4) (Zhang et al., 2025), the dataset is biased toward higher values, which partially explains the underestimation of AAOD in our simulation.

The underestimation of Abs_{365} against ATom-4data (Figure 4) and AAOD against AERONET data (Figure 5 and 6) may be reconciled by applying the newly released GFED5 fire emission inventory (https://globalfiredata.org/, Last access: 10 April, 2025), which predicts higher fire emissions than GFED4s used in our main results. However, the application of GFED5 also leads to overestimation of OA in the lower troposphere against ATom-4 data and AOD against AERONET data (Figure 4 and 6).

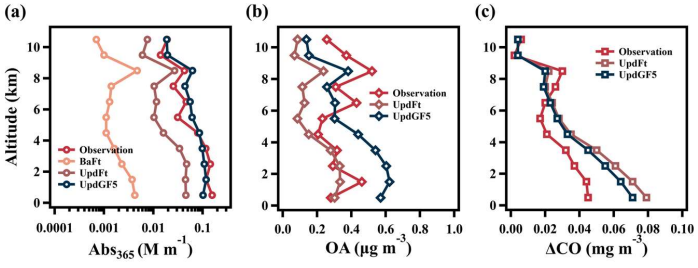

Figure 4.Vertical distribution of the median light absorption coefficient of BrC at 365 nm (a), total OA concentration (b) and ΔCO concentration (c) from simulation and observations (ATom-4). ΔCO is calculated as the CO concentration minus the background value (0.064 mg m^{-3} for observations, 0.0194 mg m^{-3} for UpdFt, and 0.0189 mg m^{-3} for UpdGF5).

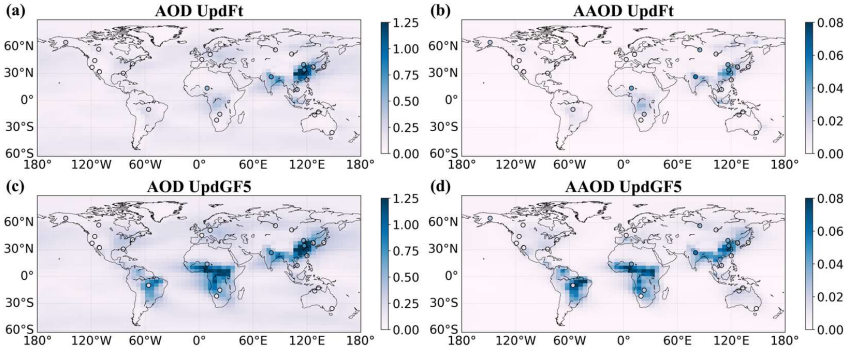

https://doi.org/10.5194/egusphere-2025-2305
Preprint. Discussion started: 28 May 2025

Figure 5. Global distribution of (a) AOD and (b) AAOD at 440 nm with updated τ_BrC. AOD (c) and AAOD with updated τ_BrC from GFED5. The dots are the observed AOD and AAOD from AERONET at 440 nm.

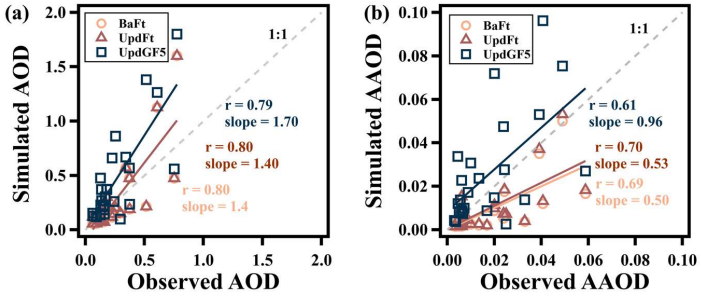

Figure 6. Linear correlation between observed and simulated AOD (a) and AAOD (b).

3.4 Direct radiative effect of BrC

The presence of BrC enhances the overall absorptivity of aerosols, leading to positive direct radiative effects (DRE) at the top of the atmosphere. Incorporating an improved τ_{BrC} parameterization into the model increases the DRE of BrC absorption from +0.059 W m^{-2} in the baseline simulation to +0.088 W m^{-2} in the UpdFT simulation (Figure 7). This 48% enhancement in DRE highlights the sensitivity of BrC's radiative effects to the rate of bleaching. Our estimate of the BrC DRE is within the estimates by previous studies (0.04 – 0.11 W m^{-2}) (Wang et al., 2018; A. Zhang et al., 2020; Feng et al., 2023) (Feng et al., 2013). The value is higher than the estimate by Wang et al. (2018) (+0.048 W m^{-2}), which did not account for longer τ_{BrC} in the cold and dry environment, but is lower than those reported by Zhang et al. (2020) (+0.10 W m^{-2}), which made an assumption that convection-lofted BrC does not photo-bleach. The light absorption of BrC reduces the negative DRE of OA by 5.7% in the baseline simulation and by 8.4% in the UpdFT simulation (Figure 7).

https://doi.org/10.5194/egusphere-2025-2305
Preprint. Discussion started: 28 May 2025

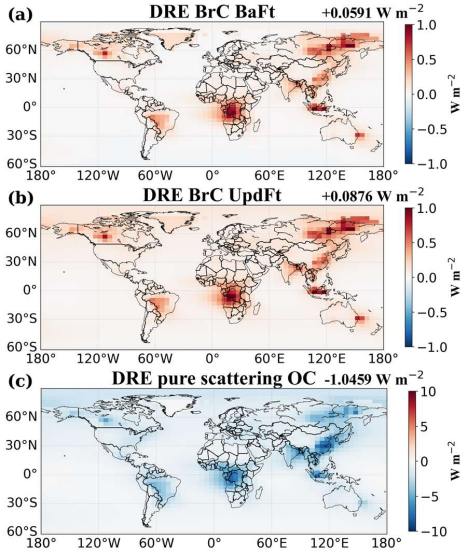

445 Figure 7. The DRE of original τ_BrC (a) and updated τ_BrC (b), and pure scattering OC (c).

3.5 Effects of BrC on atmospheric chemistry

BrC reduces the ultraviolet light available for photochemical reactions, affecting 450 atmospheric chemistry. Figure 8 evaluates the effect of BrC light absorption on the photolysis rate of NO_2 (JNO_2) and concentrations of O_3 and OH radicals. The effects are most pronounced in regions with substantial biomass burning emissions. The annual average of JNO_2 decreases by 0 – 7.4%, while surface ozone levels decline by 0 – 2.5%. These results are consistent with, but slightly lower than the results of Jo et al. (2016). 455 The light absorption of BrC also results in a 0 – 6.9% reduction in tropospheric OH concentration, which is also lower than those reported in the Northern Hemisphere in Jo et al. (2016) (0 – 10%) and Jiang et al. (2012) (up to 15%).

The effects of BrC on atmospheric chemistry are more substantial in the season and 460 region with intensive biomass burning. For instance, the reduction in JNO_2 and surface ozone concentration due to BrC reached 36.3% and 4 ppb (17.5%), respectively, in high latitude Siberia, Russia in August 2019 (Figure S5), when a large wildfire event

https://doi.org/10.5194/egusphere-2025-2305
Preprint. Discussion started: 28 May 2025

occurred (Konovalov et al., 2021a; Konovalov et al., 2021b). Another example is the large wildfire over tropical Malaysia in September 2019, which accounted for approximately 40% of its annual total wildfire emissions. In this case, JNO_2 decreased by about 27.6%, and surface O_3 concentrations by as much as 6.4 ppb (10.8%) (Figure S6).

Figure S7 shows the overall responses of atmospheric chemistry to wildfire emissions including reactive gases and aerosols. Wildfire emissions increase tropospheric ozone concentrations, while increasing OH concentrations near fire sources and suppressing OH concentrations away from the source. Comparison of Figure S8 and Figure 8 indicates that the inclusion of BrC light absorption suppresses the ozone enhancement and near-source OH enhancement, but amplifies OH reduction due to wildfires by ~12%, suggesting that ignoring the light absorption of BrC in the model incurs moderate biases in predicting chemical responses to wildfire emissions.

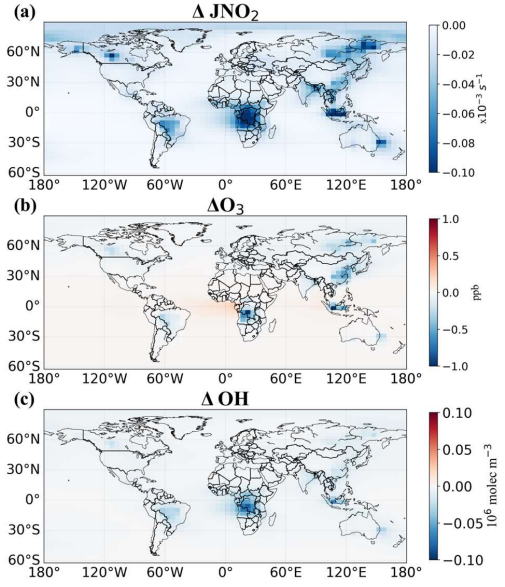

Figure 8. The effect of BrC absorption on global surface photolysis rates JNO_2 (a), O_3 (b), and column OH (c).

https://doi.org/10.5194/egusphere-2025-2305
Preprint. Discussion started: 28 May 2025

Conclusions

This study implements an updated τ_{BrC} parameterization developed by Schnitzler et al. (2022) in the GEOS-Chem model and evaluates its impact on BrC's radiative and chemical effects. τ_{BrC} is parameterized to strongly depend on temperature and relative humidity. This results in τ_{BrC} that varies by orders of magnitude, from just a few hours in warm, humid boundary layers to over 2 weeks in cold, dry upper atmospheres. In contrast, the original parameterization in the model is a weak function of OH concentration and thus rather uniform throughout the troposphere.

Compared to the original parameterization, the revised τ_{BrC} increases the global average BrC lifetime from 0.45 to 1.45 days, leading to a tripling of global fresh BrC burdens. The revised τ_{BrC} also leads to higher BrC concentrations in the middle and upper troposphere, particularly evident over source regions with deep convective activity, such as Central Africa and South Asia. In addition, injecting fire emissions into the free troposphere increases fresh BrC burdens by 30-50% relative to surface-only emissions, highlighting the interplay between fire injection and BrC persistence.

The updated τ_{BrC} parameterization improves the agreement between simulation and observations, particularly in the upper troposphere, but still generally underestimates BrC absorption (Abs_{365}) in the ATom-4 campaign and AAOD in AERONET biomass burning regions. Using GFED5 fire emission inventory, which has higher wildfire emissions, instead of GFED4s, can address these underestimations, but leads to overestimations in OA and AOD.

The revised bleaching lifetimes lead to a 48% increase in BrC's global direct radiative effect from +0.059 to +0.088 W m^{-2} compared to conventional fixed-lifetime approaches. BrC DRE surpasses BC DRE in regions with significant biomass burning,

https://doi.org/10.5194/egusphere-2025-2305
Preprint. Discussion started: 28 May 2025

underlining its important role in the regional radiation budget and its contribution to canceling out the negative DRE of OA.

In addition, the light absorption of BrC influences atmospheric chemistry by reducing the JNO_2 rate (0-7.4%), surface ozone concentrations (0 – 2.5%), and tropospheric OH concentrations (0 – 6.9%). The strongest effects were observed during intense wildfire events, with decreases of more than 36% in JNO_2 and more than 17% in ozone. In addition, BrC can suppress the enhancement of ozone and OH near wildfires, but amplifying OH decreases (12%) distant from the sources, demonstrating its role in regulating atmospheric responses to wildfires.

Author contributions. XCX and YZZ conceived and designed the study. XCX performed all model simulations and data analyses, produced all figures, and wrote the manuscript. RSL assisted with coding issues that arose during the study. YZZ revised the manuscript and other authors contributed to the improvement of the draft. All model development was performed by XCX under the guidance of YZZ and XW.

Acknowledgement

This work was supported by the National Natural Science Foundation of China (42275112). The authors thank the High-Performance Computing Center of Westlake University and the National Supercomputing Center at Wuxi for facility support and technical assistance. We thank Elijah Schnitzler for his valuable work, which provided important insights for this study.

References

The International GEOS-Chem User Community.(2020) geoschem/geos-chem: GEOS-Chem (12.8.2). https://doi.org/10.5281/zenodo.3860693, last access: may 27.

2011 National Emissions Inventory (NEI) Data: https://www.epa.gov/air-emissions-inventories/2011-national-emissions-inventory-nei-data, last access: may 27.

https://doi.org/10.5194/egusphere-2025-2305
Preprint. Discussion started: 28 May 2025

Andreae, M. O. and Gelencsér, A.: Black carbon or brown carbon? The nature of light-absorbing carbonaceous aerosols, Atmos Chem Phys, 6, 3131-3148, 10.5194/acp-6-3131-2006, 2006.

Andreae, M. O. and Merlet, P.: Emission of trace gases and aerosols from biomass burning, Global Biogeochemical Cycles, 15, 955-966, 10.1029/2000gb001382, 2001.

Bond, T. C., Bhardwaj, E., Dong, R., Jogani, R., Jung, S., Roden, C., Streets, D. G., and Trautmann, N. M.: Historical emissions of black and organic carbon aerosol from energy-related combustion, 1850-2000, Global Biogeochemical Cycles, 21, 1-16, 10.1029/2006gb002840, 2007.

Brown, H., Liu, X., Feng, Y., Jiang, Y., Wu, M., Lu, Z., Wu, C., Murphy, S., and Pokhrel, R.: Radiative effect and climate impacts of brown carbon with the Community Atmosphere Model (CAM5), Atmos Chem Phys, 18, 17745-17768, 10.5194/acp-18-17745-2018, 2018.

Burke, M., Childs, M. L., de la Cuesta, B., Qiu, M., Li, J., Gould, C. F., Heft-Neal, S., and Wara, M.: The contribution of wildfire to PM(2.5) trends in the USA, Nature, 622, 761-766, 10.1038/s41586-023-06522-6, 2023.

Canada's Air Pollutant Emissions Inventory: https://Canada.ca/APEI, last access may 27.

Chen, Y., Xie, X., Shi, Z., Li, Y., Gai, X., Wang, J., Li, H., Wu, Y., Zhao, X., Chen, M., and Ge, X.: Brown carbon in atmospheric fine particles in Yangzhou, China: Light absorption properties and source apportionment, Atmospheric Research, 244, 105028, 10.1016/j.atmosres.2020.105028, 2020.

Chung, C. E., Ramanathan, V., and Decremer, D.: Observationally constrained estimates of carbonaceous aerosol radiative forcing, Proc Natl Acad Sci U S A, 109, 11624-11629, 10.1073/pnas.1203707109, 2012.

Collow, A. B., Colarco, P. R., da Silva, A. M., Buchard, V., Bian, H., Chin, M., Das, S., Govindaraju, R., Kim, D., and Aquila, V.: Benchmarking GOCART-2G in the Goddard Earth Observing System (GEOS), Geoscientific Model Development, 17,

https://doi.org/10.5194/egusphere-2025-2305
Preprint. Discussion started: 28 May 2025

1443-1468, 10.5194/gmd-17-1443-2024, 2024.

Crippa, M., Guizzardi, D., Muntean, M., Schaaf, E., Dentener, F., van Aardenne, J. A., Monni, S., Doering, U., Olivier, J. G. J., Pagliari, V., and Janssens-Maenhout, G.: Gridded emissions of air pollutants for the period 1970–2012 within EDGAR v4.3.2, Earth System Science Data, 10, 1987-2013, 10.5194/essd-10-1987-2018, 2018.

Cunningham, C. X., Williamson, G. J., and Bowman, D.: Increasing frequency and intensity of the most extreme wildfires on Earth, Nat Ecol Evol, 10.1038/s41559-024-02452-2, 2024.

DeLessio, M. A., Tsigaridis, K., Bauer, S. E., Chowdhary, J., and Schuster, G. L.: Modeling atmospheric brown carbon in the GISS ModelE Earth system model, Atmos Chem Phys, 24, 6275-6304, 10.5194/acp-24-6275-2024, 2024.

Drugé, T., Nabat, P., Mallet, M., Michou, M., Rémy, S., and Dubovik, O.: Modeling radiative and climatic effects of brown carbon aerosols with the ARPEGE-Climat global climate model, Atmos Chem Phys, 22, 12167-12205, 10.5194/acp-22-12167-2022, 2022.

Dubovik, O. and King, M. D.: A flexible inversion algorithm for retrieval of aerosol optical properties from Sun and sky radiance measurements, Journal of Geophysical Research: Atmospheres, 105, 20673-20696, 10.1029/2000jd900282, 2000.

Duncan Fairlie, T., Jacob, D. J., and Park, R. J.: The impact of transpacific transport of mineral dust in the United States, Atmos Environ, 41, 1251-1266, 10.1016/j.atmosenv.2006.09.048, 2007.

Feng, Y., Ramanathan, V., and Kotamarthi, V. R.: Brown carbon: a significant atmospheric absorber of solar radiation?, Atmos Chem Phys, 13, 8607-8621, 10.5194/acp-13-8607-2013, 2013.

Forrister, H., Liu, J., Scheuer, E., Dibb, J., Ziemba, L., Thornhill, K. L., Anderson, B., Diskin, G., Perring, A. E., Schwarz, J. P., Campuzano-Jost, P., Day, D. A., Palm, B. B., Jimenez, J. L., Nenes, A., and Weber, R. J.: Evolution of brown carbon in

https://doi.org/10.5194/egusphere-2025-2305
Preprint. Discussion started: 28 May 2025

wildfire plumes, Geophys Res Lett, 42, 4623-4630, 10.1002/2015gl063897, 2015.

Fountoukis, C. and Nenes, A.: ISORROPIA II: a computationally efficient thermodynamic equilibrium model for K+–Ca2+–Mg2+–NH+4 –Na+–SO2− 4 – NO− 3 –Cl−–H2O aerosols, Atmos Chem Phys, 7, 4639–4659, 10.5194/acp-7-4639-2007, 2007.

Fu, X., Wang, S., Zhao, B., Xing, J., Cheng, Z., Liu, H., and Hao, J.: Emission inventory of primary pollutants and chemical speciation in 2010 for the Yangtze River Delta region, China, Atmos Environ, 70, 39-50, 10.1016/j.atmosenv.2012.12.034, 2013.

Gelaro, R., McCarty, W., Suarez, M. J., Todling, R., Molod, A., Takacs, L., Randles, C., Darmenov, A., Bosilovich, M. G., Reichle, R., Wargan, K., Coy, L., Cullather, R., Draper, C., Akella, S., Buchard, V., Conaty, A., da Silva, A., Gu, W., Kim, G. K., Koster, R., Lucchesi, R., Merkova, D., Nielsen, J. E., Partyka, G., Pawson, S., Putman, W., Rienecker, M., Schubert, S. D., Sienkiewicz, M., and Zhao, B.: The Modern-Era Retrospective Analysis for Research and Applications, Version 2 (MERRA-2), J Clim, Volume 30, 5419-5454, 10.1175/JCLI-D-16-0758.1, 2017.

Giglio, L., Randerson, J. T., and van der Werf, G. R.: Analysis of daily, monthly, and annual burned area using the fourth-generation global fire emissions database (GFED4), Journal of Geophysical Research: Biogeosciences, 118, 317-328, 10.1002/jgrg.20042, 2013.

Giles, D. M., Sinyuk, A., Sorokin, M. G., Schafer, J. S., Smirnov, A., Slutsker, I., Eck, T. F., Holben, B. N., Lewis, J. R., Campbell, J. R., Welton, E. J., Korkin, S. V., and Lyapustin, A. I.: Advancements in the Aerosol Robotic Network (AERONET) Version 3 database – automated near-real-time quality control algorithm with improved cloud screening for Sun photometer aerosol optical depth (AOD) measurements, Atmos Meas Tech, 12, 169-209, 10.5194/amt-12-169-2019, 2019.

Hammer, M. S., Martin, R. V., van Donkelaar, A., Buchard, V., Torres, O., Ridley, D. A., and Spurr, R. J. D.: Interpreting the ultraviolet aerosol index observed with the OMI satellite instrument to understand absorption by organic aerosols: implications for atmospheric oxidation and direct radiative effects, Atmos Chem

https://doi.org/10.5194/egusphere-2025-2305
Preprint. Discussion started: 28 May 2025

Phys, 16, 2507-2523, 10.5194/acp-16-2507-2016, 2016.

Heald, C. L., Ridley, D. A., Kroll, J. H., Barrett, S. R. H., Cady-Pereira, K. E., Alvarado, M. J., and Holmes, C. D.: Contrasting the direct radiative effect and direct radiative forcing of aerosols, Atmos Chem Phys, 14, 5513-5527, 10.5194/acp-14-5513-2014, 2014.

Holben, B. N., Eck, T., Slutsker, I., Smirnov, A., Sinyuk, A., Schafer, J., Giles, D., and Dubovik, O.: AERONET's Version 2.0 quality assurance criteria, https://doi.org/10.1117/12.706524,, 2006.

Huang, X., Ding, K., Liu, J., Wang, Z., Tang, R., Xue, L., Wang, H., Zhang, Q., Tan, Z.-M., Fu, C., Davis, S. J., Andreae, M. O., and Ding, A.: Smoke-weather interaction affects extreme wildfires in diverse coastal regions, Science, 379, 457–461, 2023.

Jaeglé, L., Quinn, P. K., Bates, T. S., Alexander, B., and Lin, J. T.: Global distribution of sea salt aerosols: new constraints from in situ and remote sensing observations, Atmos Chem Phys, 11, 3137-3157, 10.5194/acp-11-3137-2011, 2011.

Jiang, X., Wiedinmyer, C., and Carlton, A. G.: Aerosols from fires: an examination of the effects on ozone photochemistry in the Western United States, Environ Sci Technol, 46, 11878-11886, 10.1021/es301541k, 2012.

Jo, D. S., Park, R. J., Lee, S., Kim, S.-W., and Zhang, X.: A global simulation of brown carbon: implications for photochemistry and direct radiative effect, Atmos Chem Phys, 16, 3413-3432, 10.5194/acp-16-3413-2016, 2016.

Jolly, W. M., Cochrane, M. A., Freeborn, P. H., Holden, Z. A., Brown, T. J., Williamson, G. J., and Bowman, D. M.: Climate-induced variations in global wildfire danger from 1979 to 2013, Nat Commun, 6, 7537, 10.1038/ncomms8537, 2015.

Kelesidis, G. A., Neubauer, D., Fan, L. S., Lohmann, U., and Pratsinis, S. E.: Enhanced Light Absorption and Radiative Forcing by Black Carbon Agglomerates, Environ Sci Technol, 56, 8610-8618, 10.1021/acs.est.2c00428, 2022.

Kim, P. S., Jacob, D. J., Fisher, J. A., Travis, K., Yu, K., Zhu, L., Yantosca, R. M., Sulprizio, M. P., Jimenez, J. L., Campuzano-Jost, P., Froyd, K. D., Liao, J., Hair,

https://doi.org/10.5194/egusphere-2025-2305
Preprint. Discussion started: 28 May 2025

J. W., Fenn, M. A., Butler, C. F., Wagner, N. L., Gordon, T. D., Welti, A., Wennberg, P. O., Crounse, J. D., St. Clair, J. M., Teng, A. P., Millet, D. B., Schwarz, J. P., Markovic, M. Z., and Perring, A. E.: Sources, seasonality, and trends of southeast US aerosol: an integrated analysis of surface, aircraft, and satellite observations with the GEOS-Chem chemical transport model, Atmos Chem Phys, 15, 10411-10433, 10.5194/acp-15-10411-2015, 2015.

Konovalov, I. B., Golovushkin, N. A., Beekmann, M., and Andreae, M. O.: Insights into the aging of biomass burning aerosol from satellite observations and 3D atmospheric modeling: evolution of the aerosol optical properties in Siberian wildfire plumes, Atmos Chem Phys, 21, 357-392, 10.5194/acp-21-357-2021, 2021a.

Konovalov, I. B., Golovushkin, N. A., Beekmann, M., Panchenko, M. V., and Andreae, M. O.: Inferring the absorption properties of organic aerosol in biomass burning plumes from remote optical observations, atmospheric measurement Techniques Discussions, 10.5194/amt-2021-151, 2021b.

Lack, D. A. and Langridge, J. M.: On the attribution of black and brown carbon light absorption using the Ångström exponent, Atmos Chem Phys, 13, 10535-10543, 10.5194/acp-13-10535-2013, 2013.

Laskin, A., Laskin, J., and Nizkorodov, S. A.: Chemistry of atmospheric brown carbon, Chem Rev, 115, 4335-4382, 10.1021/cr5006167, 2015.

Li, C., van Donkelaar, A., Hammer, M. S., McDuffie, E. E., Burnett, R. T., Spadaro, J. V., Chatterjee, D., Cohen, A. J., Apte, J. S., Southerland, V. A., Anenberg, S. C., Brauer, M., and Martin, R. V.: Reversal of trends in global fine particulate matter air pollution, Nat Commun, 14, 5349, 10.1038/s41467-023-41086-z, 2023.

Li, M., Zhang, Q., Kurokawa, J. I., Woo, J. H., He, K. B., Lu, Z. F., Ohara, T., Song, Y., Streets, D. G., Carmichael, G. R., Cheng, Y. F., Hong, C. P., Huo, H., Jiang, X. J., Kang, S. C., Liu, F., Su, H., and Zheng, B.: MIX: a mosaic Asian anthropogenic emission inventory under the international collaboration framework of the MICS-Asia and HTAP, Atmos Chem Phys, 17, 935-963, 10.5194/acp-17-935-2017, 2017.

https://doi.org/10.5194/egusphere-2025-2305
Preprint. Discussion started: 28 May 2025

Lin, P., Bluvshtein, N., Rudich, Y., Nizkorodov, S. A., Laskin, J., and Laskin, A.: Molecular Chemistry of Atmospheric Brown Carbon Inferred from a Nationwide Biomass Burning Event, Environ Sci Technol, 51, 11561-11570, 10.1021/acs.est.7b02276, 2017.

Liu, J., Bergin, M., Guo, H., King, L., Kotra, N., Edgerton, E., and Weber, R. J.: Size-resolved measurements of brown carbon in water and methanol extracts and estimates of their contribution to ambient fine-particle light absorption, Atmos Chem Phys, 13, 12389-12404, 10.5194/acp-13-12389-2013, 2013.

Liu, J., Scheuer, E., Dibb, J., Ziemba, L. D., Thornhill, K. L., Anderson, B. E., Wisthaler, A., Mikoviny, T., Devi, J. J., Bergin, M., and Weber, R. J.: Brown Carbon in the Continental Troposphere, Geophys Res Lett, 2013GL058976, 10.1002/2013GL058976, 2014.

Marais, E. A. and Wiedinmyer, C.: Air Quality Impact of Diffuse and Inefficient Combustion Emissions in Africa (DICE-Africa), Environ Sci Technol, 50, 10739-10745, 10.1021/acs.est.6b02602, 2016.

Park, R. J.: Sources of carbonaceous aerosols over the United States and implications for natural visibility, J Geophys Res 108, 10.1029/2002jd003190, 2003.

Prather, M. J., Zhu, X., Flynn, C. M., Strode, S. A., Rodriguez, J. M., Steenrod, S. D., Liu, J., Lamarque, J.-F., Fiore, A. M., Horowitz, L. W., Mao, J., Murray, L. T., Shindell, D. T., and Wofsy, S. C.: Global atmospheric chemistry – which air matters, Atmos Chem Phys, 17, 9081-9102, 10.5194/acp-17-9081-2017, 2017.

Pye, H. O. T., Chan, A. W. H., Barkley, M. P., and Seinfeld, J. H.: Global modeling of organic aerosol: the importance of reactive nitrogen (NOx and NO3), Atmos Chem Phys, 10, 11261-11276, 10.5194/acp-10-11261-2010, 2010.

Randerson, J. T., Van Der Werf, G. R., Giglio, L., Collatz, G. J., and Kasibhatla, P. S.: Global Fire Emissions Database, Version 4.1 (GFEDv4), https://doi.org/10.3334/ornldaac/1293 2017.

Saleh, R., Robinson, E. S., Tkacik, D. S., Ahern, A. T., Liu, S., Aiken, A. C., Sullivan, R. C., Presto, A. A., Dubey, M. K., Yokelson, R. J., Donahue, N. M., and Robinson,

https://doi.org/10.5194/egusphere-2025-2305
Preprint. Discussion started: 28 May 2025

A. L.: Brownness of organics in aerosols from biomass burning linked to their black carbon content, Nature Geoscience, 7, 647-650, 10.1038/ngeo2220

Schnitzler, E. G., Gerrebos, N. G. A., Carter, T. S., Huang, Y., Heald, C. L., Bertram, A. K., and Abbatt, J. P. D.: Rate of atmospheric brown carbon whitening governed by environmental conditions, Proc Natl Acad Sci U S A, 119, e2205610119, 10.1073/pnas.2205610119, 2022.

Selimovic, V., Yokelson, R. J., McMeeking, G. R., and Coefield, S.: Aerosol mass and optical properties, smoke influence on O3, and high NO3 production rates in a western US city impacted by wildfires, Journal of Geophysical Research: Atmospheres, 10.1029/2020jd032791, 2020.

Shah, V., Jacob, D. J., Li, K., Silvern, R. F., Zhai, S., Liu, M., Lin, J., and Zhang, Q.: Effect of changing NOx lifetime on the seasonality and long-term trends of satellite-observed tropospheric NO2 columns over China, Atmos Chem Phys, 20, 1483-1495, 10.5194/acp-20-1483-2020, 2020.

Shao, J., Chen, Q., Wang, Y., Lu, X., He, P., Sun, Y., Shah, V., Martin, R. V., Philip, S., Song, S., Zhao, Y., Xie, Z., Zhang, L., and Alexander, B.: Heterogeneous sulfate aerosol formation mechanisms during wintertime Chinese haze events: air quality model assessment using observations of sulfate oxygen isotopes in Beijing, Atmos Chem Phys, 19, 6107-6123, 10.5194/acp-19-6107-2019, 2019.

Srinivas, B., Rastogi, N., Sarin, M. M., Singh, A., and Singh, D.: Mass absorption efficiency of light absorbing organic aerosols from source region of paddy-residue burning emissions in the Indo-Gangetic Plain, Atmos Environ, 125, 360-370, 10.1016/j.atmosenv.2015.07.017, 2016.

Thapa, L. H., Ye, X., Hair, J. W., Fenn, M. A., Shingler, T., Kondragunta, S., Ichoku, C., Dominguez, R., Ellison, L., Soja, A. J., Gargulinski, E., Ahmadov, R., James, E., Grell, G. A., Freitas, S. R., Pereira, G., and Saide, P. E.: Heat flux assumptions contribute to overestimation of wildfire smoke injection into the free troposphere, Communications Earth & Environment, 3, 10.1038/s43247-022-00563-x, 2022.

Thompson, C. R., Wofsy, S. C., Prather, M. J., Newman, P. A., Hanisco, T. F., Ryerson,

https://doi.org/10.5194/egusphere-2025-2305
Preprint. Discussion started: 28 May 2025

T. B., Fahey, D. W., Apel, E. C., Brock, C. A., Brune, W. H., Froyd, K., Katich, J. M., Nicely, J. M., Peischl, J., Ray, E., Veres, P. R., Wang, S., Allen, H. M., Asher, E., Bian, H., Blake, D., Bourgeois, I., Budney, J., Bui, T. P., Butler, A., Campuzano-Jost, P., Chang, C., Chin, M., Commane, R., Correa, G., Crounse, J. D., Daube, B., Dibb, J. E., DiGangi, J. P., Diskin, G. S., Dollner, M., Elkins, J. W., Fiore, A. M., Flynn, C. M., Guo, H., Hall, S. R., Hannun, R. A., Hills, A., Hintsa, E. J., Hodzic, A., Hornbrook, R. S., Huey, L. G., Jimenez, J. L., Keeling, R. F., Kim, M. J., Kupc, A., Lacey, F., Lait, L. R., Lamarque, J.-F., Liu, J., McKain, K., Meinardi, S., Miller, D. O., Montzka, S. A., Moore, F. L., Morgan, E. J., Murphy, D. M., Murray, L. T., Nault, B. A., Neuman, J. A., Nguyen, L., Gonzalez, Y., Rollins, A., Rosenlof, K., Sargent, M., Schill, G., Schwarz, J. P., Clair, J. M. S., Steenrod, S. D., Stephens, B. B., Strahan, S. E., Strode, S. A., Sweeney, C., Thames, A. B., Ullmann, K., Wagner, N., Weber, R., Weinzierl, B., Wennberg, P. O., Williamson, C. J., Wolfe, G. M., and Zeng, L.: The NASA Atmospheric Tomography (ATom) Mission: Imaging the Chemistry of the Global Atmosphere, Bulletin of the American Meteorological Society, 103, E761-E790, 10.1175/bams-d-20-0315.1, 2022.

van der Werf, G. R., Randerson, J. T., Giglio, L., van Leeuwen, T. T., Chen, Y., Rogers, B. M., Mu, M., van Marle, M. J. E., Morton, D. C., Collatz, G. J., Yokelson, R. J., and Kasibhatla, P. S.: Global fire emissions estimates during 1997–2016, Earth Syst Sci Data, 9, 697-720, 10.5194/essd-9-697-2017, 2017.

Wang, X., Heald, C. L., Liu, J., Weber, R. J., Campuzano-Jost, P., Jimenez, J. L., Schwarz, J. P., and Perring, A. E.: Exploring the observational constraints on the simulation of brown carbon, Atmos Chem Phys, 18, 635-653, 10.5194/acp-18-635-2018, 2018.

Wang, X., Heald, C. L., Ridley, D. A., Schwarz, J. P., Spackman, J. R., Perring, A. E., Coe, H., Liu, D., and Clarke, A. D.: Exploiting simultaneous observational constraints on mass and absorption to estimate the global direct radiative forcing of black carbon and brown carbon, Atmos Chem Phys, 14, 10989-11010,

https://doi.org/10.5194/egusphere-2025-2305
Preprint. Discussion started: 28 May 2025

10.5194/acp-14-10989-2014, 2014.

Washenfelder, R. A., Attwood, A. R., Brock, C. A., Guo, H., Xu, L., Weber, R. J., Ng, N. L., Allen, H. M., Ayres, B. R., Baumann, K., Cohen, R. C., Draper, D. C., Duffey, K. C., Edgerton, E., Fry, J. L., Hu, W. W., Jimenez, J. L., Palm, B. B., Romer, P., Stone, E. A., Wooldridge, P. J., and Brown, S. S.: Biomass burning dominates brown carbon absorption in the rural southeastern United States, Geophys Res Lett, 42, 653-664, 10.1002/2014gl062444, 2015.

Wu, G., Ram, K., Fu, P., Wang, W., Zhang, Y., Liu, X., Stone, E. A., Pradhan, B. B., Dangol, P. M., Panday, A., Wan, X., Bai, Z. P., Kang, S., Zhang, Q., and Cong, Z.: Water-Soluble Brown Carbon in Atmospheric Aerosols from Godavari (Nepal), a Regional Representative of South Asia, Environ Sci Technol, 53, 3471-3479, 10.1021/acs.est.9b00596, 2019.

Xu, L., Lin, G., Liu, X., Wu, C., Wu, Y., and Lou, S.: Constraining Light Absorption of Brown Carbon in China and Implications for Aerosol Direct Radiative Effect, Geophys Res Lett, 51, 10.1029/2024gl109861, 2024.

Yan, C., Zheng, M., Bosch, C., Andersson, A., Desyaterik, Y., Sullivan, A. P., Collett, J. L., Zhao, B., Wang, S., He, K., and Gustafsson, O.: Important fossil source contribution to brown carbon in Beijing during winter, Scientific reports, 7, 43182, 10.1038/srep43182, 2017.

Yue, S., Zhu, J., Chen, S., Xie, Q., Li, W., Li, L., Ren, H., Su, S., Li, P., Ma, H., Fan, Y., Cheng, B., Wu, L., Deng, J., Hu, W., Ren, L., Wei, L., Zhao, W., Tian, Y., Pan, X., Sun, Y., Wang, Z., Wu, F., Liu, C.-Q., Su, H., Penner, J. E., Pöschl, U., Andreae, M. O., Cheng, Y., and Fu, P.: Brown carbon from biomass burning imposes strong circum-Arctic warming, One Earth, 5, 293-304, 10.1016/j.oneear.2022.02.006, 2022.

Zeng, L., Zhang, A., Wang, Y., Wagner, N. L., Katich, J. M., Schwarz, J. P., Schill, G. P., Brock, C., Froyd, K. D., Murphy, D. M., Williamson, C. J., Kupc, A., Scheuer, E., Dibb, J., and Weber, R. J.: Global Measurements of Brown Carbon and Estimated Direct Radiative Effects, Geophys Res Lett, 47, e2020GL088747,

https://doi.org/10.5194/egusphere-2025-2305
Preprint. Discussion started: 28 May 2025

10.1029/2020GL088747, 2020.

Zhang, A., Wang, Y., Zhang, Y., Weber, R. J., Song, Y., Ke, Z., and Zou, Y.: Modeling the global radiative effect of brown carbon: a potentially larger heating source in the tropical free troposphere than black carbon, Atmos Chem Phys, 20, 1901-1920, 10.5194/acp-20-1901-2020, 2020.

Zhang, Y., Forrister, H., Liu, J., Dibb, J., Anderson, B., Schwarz, J. P., Perring, A. E., Jimenez, J. L., Campuzano-Jost, P., Wang, Y., Nenes, A., and Weber, R. J.: Top-of-atmosphere radiative forcing affected by brown carbon in the upper troposphere, Nature Geoscience, 10, 486-489, 10.1038/ngeo2960, 2017.

Zhang, Z., Li, J., Che, H., Dong, Y., Dubovik, O., Eck, T., Gupta, P., Holben, B., Kim, J., Lind, E., Saud, T., Tripathi, S. N., and Ying, T.: Long-term trends in aerosol properties derived from AERONET measurements, Atmos Chem Phys, 25, 4617-4637, 10.5194/acp-25-4617-2025, 2025.

Zheng B, Ciais P, Chevallier F, Yang H, Canadell JG, Chen Y, van der Velde IR, Aben I, Chuvieco E, Davis SJ, Deeter M, Hong C, Kong Y, Li H, Li H, Lin X, He K, and Q., Z.: Record-high CO2 emissions from boreal fires in 2021, Science, 379, 912-917, 10.1126/science.ade0805, 2023